buildings

MDPI

Article

A Simplified Approach for the Seismic Loss Assessment of RC Buildings at Urban Scale: The Case Study of Potenza (Italy)

Amedeo Flora *, Donatello Cardone, Marco Vona and Giuseppe Perrone

School of Engineering, University of Basilicata, Viale dell'Ateneo Lucano 10, 85100 Potenza, Italy; donatello.cardone@unibas.it (D.C.); marco.vona@unibas.it (M.V.); giuseppe.perrone@alice.it (G.P.)
* Correspondence: amedeo.flora@unibas.it

Abstract: Comprehensive methodologies based on a fully probabilistic approach (i.e., the performance-based earthquake engineering approach, PBEE), represent a refined and accurate tool for the seismic performance assessment of structures. However, those procedures are suitable for building-specific evaluations, appearing extremely time-consuming if applied at the urban scale. In the proposed contribution, simplified loss assessment procedure will be applied at the urban scale with reference to the residential building stock of the center of Potenza. After the identification of the main reinforced concrete (RC) structural typologies and the definition of specific archetype building numerical models, the direct estimation of expected annual loss (DEAL) methodology will be applied to derive the EAL (i.e., expected annual loss) of RC buildings, deriving information on the effectively seismic quality (or seismic resilience) of the aforementioned built heritage at urban scale. Similarly, the monetary losses associated with downtime are evaluated. Preliminary considerations on the socio-economic effects of seismic scenarios on the territorial scale are also proposed.

Keywords: seismic performance assessment; direct and indirect losses; RC frame buildings; seismic resilience; socio-economic impacts of seismic scenarios

Citation: Flora, A.; Cardone, D.; Vona, M.; Perrone, G. A Simplified Approach for the Seismic Loss Assessment of RC Buildings at Urban Scale: The Case Study of Potenza (Italy). *Buildings* **2021**, *11*, 142. https://doi.org/10.3390/buildings11040142

Academic Editors: Rita Bento and Ana Simões

Received: 26 February 2021
Accepted: 24 March 2021
Published: 1 April 2021

1. Introduction

Generally speaking, the seismic assessment of a building represents a powerful tool for (i) the evaluation of potential negative effects of significant seismic events occurring on a specific structure and (ii) the definition of the relevant strategies for the seismic retrofitting. The mentioned negative effects belong to different categories such as: structural and non-structural (physical) damage, direct losses associated with such damage (repair costs or reconstruction), indirect (economic) losses connected to building downtime (loss of productivity, business interruption, cost of occupants reallocation), and casualties. On the other hand, the choice of the better retrofit strategy can be properly defined based on rational criteria and building-specific considerations driven by the seismic assessment results [1–3]. In the last decades, several methodologies for the performance based-loss assessment have been proposed [4]. Among those, performance-based earthquake engineering (PBEE) methodology [5] represents the most comprehensive approach providing probabilistic estimates of seismic losses (direct and indirect). The principal output parameter of the mentioned approach is represented by the expected annual loss (EAL) [6], defined as the average economic loss expected to accrue every year in the structure, considering both the direct repair costs related to damage and the social costs associated to downtime (relocation and business interruption). Generally speaking, the lower is the value of EAL, the higher is the seismic quality of examined building. Obviously, the synthetic information expressed by these parameters represent a powerful tool for the stakeholders. In particular, the EAL estimations in both, the as-built and retrofitted configurations can be assumed as input parameters for a cost–benefit analysis, aimed at the rational choice of the optimal retrofit intervention among different options. The accurate evaluation of EAL requests the direct integration, over the site hazard curve, of the monetary losses conditioned on the assumed

intensity measure (IM) [7]. As a consequence, single intensity-based loss estimates, performed based on the results of non-linear dynamic analysis, are needed. Specific tools for the practical application of the PEER methodology have been proposed. The performance assessment calculation tool (PACT) represents a valuable mean for the rigorous estimation of EAL. However, it is worth noting that a correct application of this tool requires advanced skills in the non-linear modeling of structures as well as the definition of proper fragility functions and a detailed inventory of damageable components.

The described potentialities of an accurate seismic assessment appears even more attractive in the optic of an urban scale evaluation. Indeed, in this case, the derived synthetic global parameters (namely EAL) and the results of the eventual cost–benefit analyses could be used by the decision makers (government, public institutions, and organizations such as civil protection, etc.) to properly define the direction of their political choices. To better support decision makers, several studies have been carried out with the use of multi-criteria decision methods (MCDMs). In recent studies, MCDMs have been widely used particularly to define a prioritization list and for the selection of the optimal intervention strategies [8]. The mentioned results, together with further assessments on the potential social and economic large scale impacts (such as in the loss of the quality of life of the population, performance reduction of the critical infrastructures, etc.), are crucial elements to perform a resilience analysis as well as a pre- and post-event management at urban scale [9].

However, based on previous considerations, the inherent complexity of the PEER–PBEE methodology became unaffordable in case of an urban scale evaluation. In other words, the application of an accurate building-specific approach to all the structures composing the building stock appears computationally expensive, in particular for practitioners, and excessively time-consuming. Even classifying the structures located on a certain area in a limited number of typologies, the modeling effort remains particularly onerous, as well as the amount of input data for a proper application of PACT process.

Recently, many authors proposed simplified approaches relating the economic losses to the structural response (engineering demand parameters, EDP) derived from analysis methods within the reach of the most practicing engineers. In particular, the main simplification lies in relating a given performance level (PL) to an expected economic loss pre-defined based on the actual structural typology [10] or calculated based on specific story-based loss function [11]. The first approach is currently used within the Italian Seismic Risk Classification [12] to evaluate the "seismic quality" of existing buildings, providing a specific score system articulated in eight seismic risk classes. However, as observed by Perrone et al. (2019) [13], this approach is generally affected by a significant loss of accuracy in many cases, in particular for buildings characterized by drift/acceleration profiles or structural/non structural elements distributions sensibly different in the two main directions or along the building height. In contrast, the accurateness of the results derived using procedures based on the definition of story-based loss functions appears satisfactory [13]. In this context, Cardone et al. (2017) [14] firstly proposed a new approach, later developed by Perrone et al. 2019 [13], referred to as direct estimation of expected annual losses (DEAL). Under specific assumptions, the EAL of a single building can be evaluated using a closed-form equation, significantly reducing the complexity of a large scale seismic assessment.

All that considered, in the present paper, the DEAL approach has been applied at the urban scale for the seismic loss assessment of the city center of Potenza (southern Italy). A series of operative choices have been implemented to operatively perform the seismic assessment. First of all, the main structural and typological peculiarities of the residential RC buildings have been collected to define a general typologies inventory. In the second step, a series of case-study buildings (archetypes), each one associated with a single typology, have been defined and modeled using the Opensees Framework [15]. Successively, non-linear static analyses have been carried out on the mentioned non-linear models to derive the structural response, hence the main EDPs, representing the input data

for the application of the DEAL method, aimed at the evaluation of the EAL associated with direct losses. In the last part of the paper, an estimation of the EAL associated with indirect losses related to downtime is proposed according to the methodology presented in Cardone et al. (2019) [16]. Finally, based on the results in terms of monetary losses, preliminary considerations on the economic and social impacts of probable seismic scenarios are made. The main novelty of the present study is represented by the application of the DEAL methodology within an integrated approach, affordable for skilled practitioners and also useful to derive territorial scale considerations at different levels (stakeholders, local government, civil protection, etc.).

2. Overview of the Direct Estimation of Expected Annual Loss

The displacement-based (DB) simplified seismic loss assessment approach proposed by Cardone et al. (2020) [4] for RC structures is characterized by the following key points: (i) estimation of EDPs (i.e., floor acceleration and/or inter-story drifts profiles) through simple analysis methods, (ii) application of proper story-based loss functions for the estimation of expected losses at different performance levels, and (iii) direct calculation of EAL through a closed-form equation.

Two main assumptions have been considered in this approach: (i) linear increase of the expected monetary losses (associated with the seismic event) with the IM and (ii) linear approximation of the seismic hazard curve in log-space [17] (see Figure 1a).

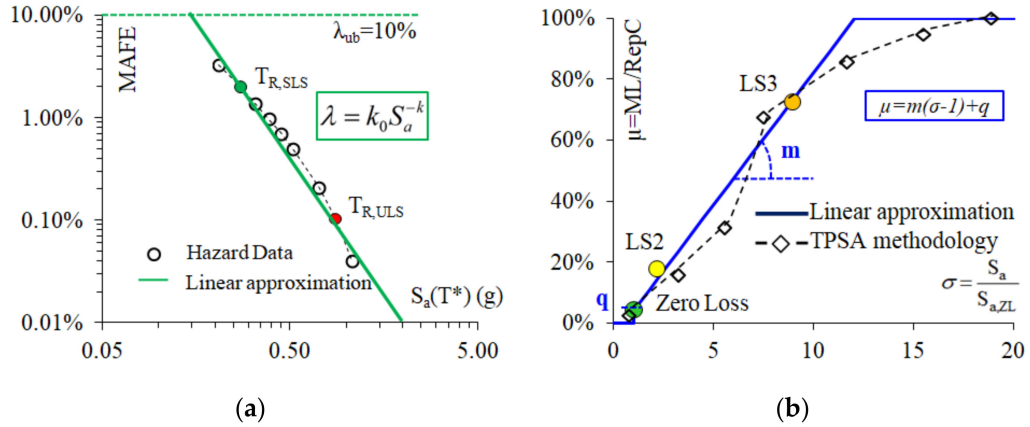

Figure 1. Assumptions of the proposed simplified procedure [4]: (**a**) hazard curve linear approximation and (**b**) expected loss vs. IM relationship.

More in detail, the hazard curve describes the mean annual frequency of exceedance (MAFE) corresponding to a certain level of ground motion as a function of the selected intensity measure, namely the spectral acceleration at the fundamental period of vibration, $S_a(T^*)$. It is worth noting that T^* is assumed equal to the mean period of vibration in the two orthogonal directions of the structure. The following relationship is used to describe the linear approximation of the hazard curve:

$$\lambda = k_0 S_a(T^*)^{-k}, \quad (1)$$

where:

$$k = [\mathrm{Log}(\lambda_{ULS}/\lambda_{SLS})]/[\mathrm{Log}(S_{a,ULS}/S_{a,SLS})], \quad (2)$$

$$k_0 = \lambda_{SLS} \times S^k{}_{a,SLS}, \quad (3)$$

with λ_{SLS} and λ_{ULS} representing the reciprocal of the return period, T_R, of earthquake at the serviceability limit state (SLS) and ultimate limit state (ULS) assumed by the current seismic code [18] and $S_{a,SLS}$ and $S_{a,ULS}$ representing the associated spectral accelerations at T^*. In order to align the DEAL approach with that provided within the Italian seismic

classification guidelines [12], a maximum value of the MAFE, namely λ_{ub} = 10% (return period equal to 10 years) has been assumed in the procedure.

As showed in [13], expected monetary losses increase almost linearly compared to the IM. In Figure 1b the loss curve of a reference RC frame building (dash-dotted line) is normalized on both axes [19]. In particular, expected monetary losses are normalized with respect to the replacement cost (RepC) of the building, while the spectral acceleration to the zero-loss seismic intensity, $S_{a,ZL}$ (IM), corresponds to a minor damage that is not going to be repaired [14]). The loss curve of the mentioned reference RC frame building has been obtained by applying the accurate time-based performance seismic assessment (TPSA) methodology proposed within FEMA P-58 [20].

All that considered, a generic story-based loss curve can be approximated using the following Equation:

$$\mu = m(s - 1) + q \leq 1, \quad (4)$$

In Equation (4), the parameter q is the initial-loss threshold corresponding to the cosmetic damage loss associated with $S_{a,ZL}$. The slope m can be obtained using a best fit regression linear approach considering other two limit states besides the zero loss point: the operational (OP) and damage control (DC) limit states. The values of $S_a(T^*)$ associated with the aforementioned limit states (ZL, OP, and DC) can be evaluated using simplified methodologies as the displacement base assessment (DBA), the MIMA approach [21], etc. On the other hand, the corresponding monetary losses can be obtained using proper story-based loss function, such as those proposed by Cardone et al. (2020) [4] for residential RC buildings. More details about the described approach can be found in [13]. Once the parameters m and q are determined, the following closed form equation can be applied to derive the direct EAL [10]:

$$EAL = \lambda_{min} q_{min} + (k_0 / S^k{}_{a,ZL}) \times [(m/(1 - k) \times (s^{1-k}{}_{TL} + s^{1-k}{}_{min})], \quad (5)$$

in which:

$$q_{min} = m(s_{min} - 1) + q, \quad (6)$$

$$s_{TL} = [(1-q)/m] + 1, \quad (7)$$

$$s_{min} = S_{a,min}/S_{a,ZL} = \max(1; S_{a,ub}/S_{a,ZL}) = \max(1; (\lambda_{ub}/k_0)^{-1/k}/S_{a,ZL})), \quad (8)$$

The parameter σ_{TL} is related to the IM value at which the normalized expected losses are equal to the 100% of RepC, λ_{ub} represents the MAFE maximum limit, σ_{min} is associated with the maximum (normalized) IM between the ZL and the spectral acceleration associated to the MAFE maximum limit ($S_{a,ub}$), and q_{min} is the corresponding monetary loss.

For what concerns the indirect component of EAL, a simplified approach has been proposed in [16]. In particular, this method takes into account the indirect losses directly associated to the interval of time between the seismic event and the end of repair activities, namely the so-called "downtime". Two main components are considered: rational and irrational. The first one represents the time needed to complete the building repair activities. Reference to a "Slow-Track" approach has been made to derive the rational component of downtime. In other words, the repair activities are performed at each floor progressively and independently from one story to another [16]. The second includes several preliminary activities: bureaucratic issues, damage assessment, financial planning, occupants relocation, technical design, etc.

Based on the mentioned approach, indirect losses vs. normalized spectral acceleration ($S_a(T^*)/S_a(T^*)_{ZL}$ relationships can be derived for a specific building. It is worth noting that a series of assumptions have been made regarding the irrational component of downtime and, in particular, regarding the relocation of buildings occupants. More in detail, in the immediate aftermath of the seismic event, building occupants are generally hosted in hotels at sub-sized rates. In a second phase, these occupants usually move to "long term" accommodations (e.g., private apartments or emergency structures). All that considered, the following assumptions have been made: (i) occupants are accommodated in hotels

considering an average cost of €40/room/day for no more than 90 days; (ii) average lease rate (C_{rental}) equal to €3.5/m^2/month [22]; (iii) average occupancy ratio equal to 1.4 persons/100 m^2 [22]. However, many factors could modify the mentioned assumptions, thus enhancing the level of uncertainty of the procedure. For example, based on the effective statistics provided by the Italian Government, the number of building occupants that effectively move to a hotel accommodation is generally lower than the total number of occupants (N_{occ}). Indeed, a part of them owns a secondary home (namely, holiday house) or is hosted by relatives. Similarly, several factors could influence the relocation time, leading to a period range variable from few days to several weeks. In this optic, two main scenarios have been defined (i.e., lower bound and upper bound conditions). In the lower bound condition, only 2/3 of the occupants are relocated. In this case, 45 days have been assumed as a relocation time. In the upper bound scenario, the totality of occupants is relocated, assuming a 90-day relocation time.

3. Building Typologies Identification for the City Center of Potenza

Potenza is the main city of the Basilicata region (southern Italy), counting about 65,000 inhabitants. The evolution of the current built heritage of Potenza is strongly related to the historical events occurred during the last two centuries.

During the XIV century, the city was hit by different significant seismic events (intensity higher than VIII MCS). Two close strong earthquakes, occurring in 1826 and 1857, produced several victims and severe damage in the entire town [23]. Important demolition and reconstruction activities were undertaken in the historical city center in the aftermath of these events [23]. In the twentieth century, a massive migration of the population from the historical city center to modern neighborhoods (in the upper west side of the city) was registered due to the demographic increment registered during the 1930s and 1940s. As a consequence, in the early 1950s, the local social housing organization funded and pursued an important public housing plan creating new residential neighborhoods. After the strong earthquake occurred on 23 November 1980 (Irpinia and Basilicata earthquake), a lot of existing buildings were retrofitted [24] using public financial resources allocated within the law 219/81.

In this paper, the seismic assessment is referred to two main areas: the old town center (located in the hilltop town, labeled as C1 in Figure 2) and the residential public housing compartment (labeled as C2). These two compartments feature homogeneous urbanistic, constructive, and historical peculiarities, including a large part of the built heritage of Potenza developed during 1850–1950 and 1945–1990, respectively. In this study, only private RC residential buildings have been considered. As a matter of fact, public buildings have been neglected due to their limited number and their inherent peculiarities deserving a specific study. As mentioned in Section 1, the building-specific approach appears extremely time consuming and computationally unfeasible for regions or areas populated by hundreds of buildings. As a consequence, the definition of a building typologies inventory represents a pragmatic choice for a simplified seismic assessment at urban-scale. Grouping buildings in limited number of typologies is an affordable operation, especially when the urban area can be divided in many sub-areas (namely compartments) characterized by similar urbanistic, historical, and constructive peculiarities.

Several criteria can be assumed for the structural typologies identification and distribution on a given area. Obviously, the consistency and completeness of the identification approach is one of the main elements affecting the accuracy of the seismic assessment. Elementary building typologies inventories are fundamentally based on the structural system construction material [25]. More advanced approaches include additional information as construction period, non-structural elements characteristics (materials and sizes), primary load bearing structure, number of stories, etc. [26]. Recently, very accurate building classification methodologies have been proposed and also incorporated in several seismic codes [27]. However, the presence and spread of a construction typology on a certain territory is generally related to many different factors, strictly connected to the inherent

peculiarities of a territory: socio-economic conditions, geological and topographical conditions, traditional building technologies, etc. In this optic, customized approaches represent a proper solution for a reliable buildings classification.

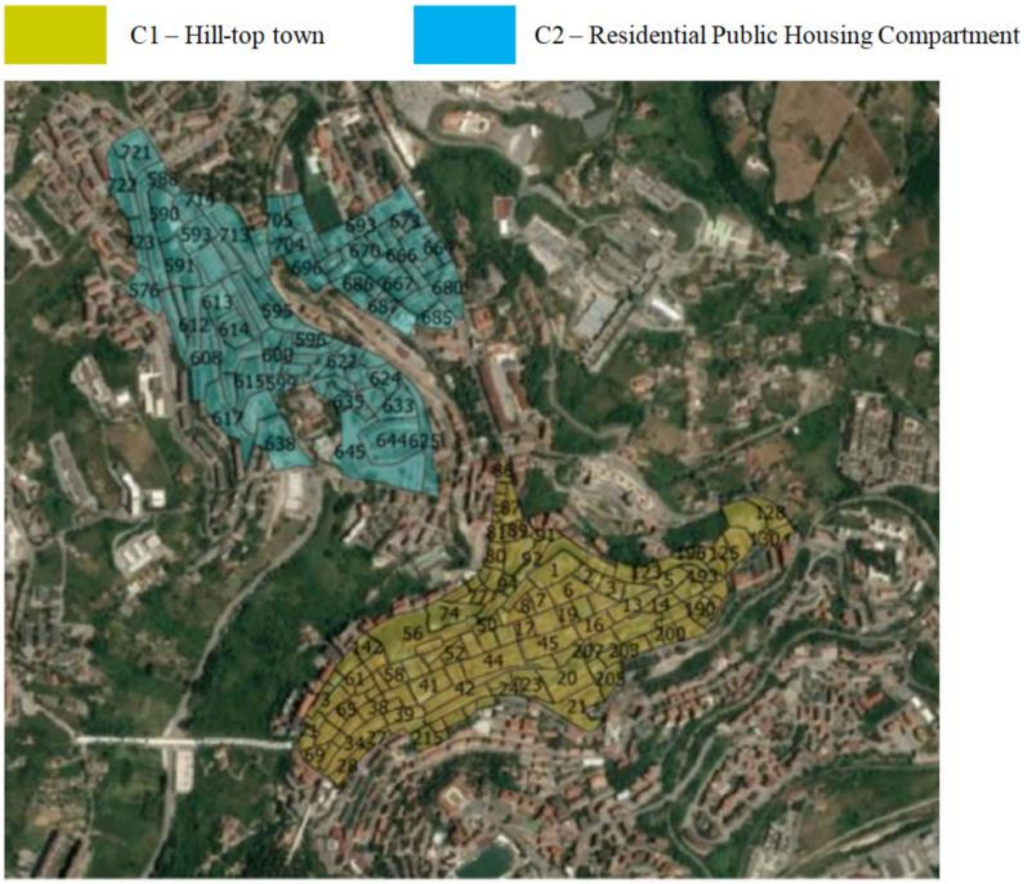

Figure 2. Compartments overview and census tracts: (yellow) old town center and (blue) residential compartments.

A typical approach for a customized classification of building typologies at territorial-scale is based on the assumption of the census database as primary source of information. Subsequently, these data (for each census tract) are integrated with other specific sources of information (in situ and virtual inspections, documental analysis, etc.) [28]. The heterogeneous data supplied by the Italian Institute of Statistics (ISTAT, [22]) appears sufficiently populated (statistics updated every 10 years) and homogeneously distributed. In Table 1, the most relevant data referring to the examined compartments derived by the ISTAT Buildings Database are summarized [22].

Table 1. Relevant data for the examined compartments.

Compartment	n° of Buildings	Masonry (Nr.(%))	RC (Nr.(%))	Pre-81 (%)	Post-81 (%)	Ns $\leq$ 3 (%)	Ns > 3 (%)
C1	429	327 (76%)	102 (24%)	90	10	49	51
C2	128	88 (69%)	40 (31%)	90	10	22	78

Based on the synthetic data reported above, two main elements emerged as significant classification variables: the number of stories (n_s) and the age of construction (a_c). Considering the aggregated form of the census data, no details are provided to directly derive more specific information as the number of RC buildings showing two, three, or more than

three stories or, similarly, how many RC structures have been realized in a certain period. For what concerns the number of stories, in order to overcome this limitation, innovative approaches, namely G.I.S. technology and high resolution (HR) optical satellite imagery, have been adopted to collect more detailed geo-referenced data on the effective height of the RC buildings in the examined territory [28], thus obtaining an adequate disaggregation of primary source data (census). With reference to n_s, three macro-classes of buildings have been identified: "Lr" (from one to three stories), "Mr" (from four to six stories), and "Hr" (from seven to 10 stories). The criterion adopted for the definition of the mentioned number of stories ranges (1–3, 4–6, and 7–10) is in line with the observation presented in Masi et al. [29]. As a matter of fact, all other variables being equal, RC buildings featuring one to three stories exhibit a similar seismic behavior [29]. The same considerations can be made for medium-rise RC buildings (four to six stories) and for high-rise buildings (seven to 10 stories).

On the other hand, two main classes have been defined with reference to the age of construction: pre- and post-1981. The identification of these classes is not merely temporal, but is associated to the reference design code. Indeed, the introduction of new seismic regulations after the Irpinia Earthquake led to enhanced anti-seismic peculiarities for buildings designed after 1981. An extensive documental investigation has been performed for the identification of the main structural peculiarities of buildings realized pre- and post-1981. A significant database furnished by the Regional Public Social Housing Organization (ATER), directly involved in the post-seismic residential reconstruction from 1981 to 1990, has been analyzed. Moreover, building inspections have been conducted gathering fundamental data on dimensional and structural peculiarities of structures sited in the examined areas.

The main structural characteristics of pre- and post-1981 buildings are resumed in what follows. For pre-1981 buildings, the typical lateral resisting system is characterized by perimeter and internal resisting frames along a single direction. Moreover, internal shallow beams and external deep beams were generally adopted. Resisting frames along both principal directions and a large use of shallow beams have been observed for post-1981 buildings. For what concerns non-structural elements, heavy masonry infills, constituted by a double layer (external 13 cm solid bricks and internal 10 cm hollow clay bricks with a 10 cm inter-space) have been observed for most of pre-1981 structures, in particular for those realized before 1961. In a few cases (in particular for buildings realized during the period 1960–1980) light masonry infills (hollow bricks positioned in two layers of 10 + 10 cm with a 10 cm inter-space) have been detected. The same configuration has been observed for post-1981 buildings.

The combination of the described peculiarities for each building class lead to a different seismic vulnerability. In this optic, a preliminary classification, in terms of seismic vulnerability, has been defined. Preliminary macro-typologies have been considered, featuring (i) low (L), (ii) medium (M), and (ii) high (H) vulnerability (see Table 2). Subsequently, the preliminary classification has been refined including specific attributes that directly affect the structural behavior. In particular, vertical irregularities and staircase typology have been taken into account. Irregularities in elevation have been observed for pre-1981 (in particular for those realized in the 1970s) and post-1981 buildings. Pilotis stories (namely open ground story) are frequent in particular in the C2 compartment. Moreover, two staircase typologies have been identified: knee beams with cantilever steps (labeled as *k* in what follows) represent the typical solution for buildings realized before 1981 and for a large part of post-1981 buildings; Waist-slab staircases (labeled as *s*) have been detected in a number cases for post-1981 buildings (in particular for those realized after 1990). The structural configurations (in plan and elevation) and the effective structural element dimensions observed during the described investigations have been properly considered in the numerical modeling (see Section 3). Negligible differences in terms of horizontal floor type, roof typology, and state of preservation have been observed.

Table 2. Preliminary macro-typologies classification.

ID	Description
L (Low)	Bi-directional lateral resisting system Light masonry infills Seismic Resistant Design
M (Medium)	Mono-directional resisting system Light masonry infills Gravity load design
H (High)	Mono- directional resisting system Heavy masonry infills Gravity load design

The final typologies inventory, resulting from the classification approach discussed above, is reported in Table 3. The theoretical total number of classes is equal to 36. However, the number of buildings effectively included in some of those classes is extremely limited. Consequently, to reduce the computational amount of the procedure and considering the low incidence of a limited number of elements on the global seismic assessment of the area, the typologies including a number of buildings lower than three have been neglected in what follows. Finally, eight typologies of the defined inventory have been effectively taken into account counting 131 buildings, distributed as reported in Table 4, thus covering the 92% of the RC residential buildings population. In other words two "virtual" compartments consisting only of residential RC buildings (afferent to the previously defined typologies) have been generated.

Table 3. Building typologies inventory.

Macro Typology			Nr. of Stories			Staircase Typolgy		Vertical Irregularities		ID
L	**M**	**H**	**Lr**	**Mr**	**Hr**	**k**	**s**	**PF**	**IF**	
x			x			x		x		L, Lr, k, PF
x			x			x			x	L, Lr, k, IF
x			x				x	x		L, Lr, s, PF
x			x				x		x	L, Lr, s, IF
x				x		x		x		L, Mr, k, PF
x				x		x			x	L, Mr, k, IF
x				x			x	x		L, Mr, s, PF
x				x			x		x	L, Mr, s, IF
x					x	x		x		L, Hr, k, PF
x					x	x			x	L, Hr, k, IF
x					x		x	x		L, Hr, s, PF
x					x		x		x	L, Hr, s, IF
	x		x			x		x		M, Lr, k, PF
	x		x			x			x	M, Lr, k, IF
	x		x				x	x		M, Lr, s, PF
	x		x				x		x	M, Lr, s, IF
	x			x		x		x		M, Mr, k, PF
	x			x		x			x	M, Mr, k, IF
	x			x			x	x		M, Mr, s, PF
	x			x			x		x	M, Mr, s, IF
	x				x	x		x		M, Hr, k, PF
	x				x	x			x	M, Hr, k, IF
	x				x		x	x		M, Hr, s, PF
	x				x		x		x	M, Hr, s, IF

Table 3. *Cont.*

Macro Typology			Nr. of Stories			Staircase Typolgy		Vertical Irregularities		ID
L	M	H	Lr	Mr	Hr	k	s	PF	IF	
		x	x			x		x		H, Lr, k, PF
		x	x			x			x	H, Lr, k, IF
		x	x				x	x		H, Lr, s, PF
		x	x				x		x	H, Lr, s, IF
		x		x		x		x		H, Mr, k, PF
		x		x		x			x	H, Mr, k, IF
		x		x			x	x		H, Mr, s, PF
		x		x			x		x	H, Mr, s, IF
		x			x	x		x		H, Hr, k, PF
		x			x	x			x	H, Hr, k, IF
		x			x		x	x		H, Hr, s, PF
		x			x		x		x	H, Hr, s, IF

Table 4. Prevalent building typologies distribution on the examined area.

Building Typology	Number of Elements	RepC (€)
L, Hr, s, IF	7	2,858,000
L, Mr, s, IF	5	2,135,000
M, Hr, k, IF	25	2,858,000
M, Mr, k, IF	22	2,135,000
M, Lr, k, IF	6	1,077,640
H, Hr, k, IF	14	2,858,000
H, Mr, k, PF	12	2,135,000
H, Mr, k, IF	40	2,135,000
Total	131	-

4. Archetype Buildings

4.1. Overview

Once the prevalent building typologies have been detected for the two compartments, a series of archetype buildings, one for each typology, is defined. Such archetypes represent, on average, the geometrical, material, and structural peculiarities of the corresponding typological class. Considering that few differences have been registered in terms of building layout, the same plan configuration has been assumed for all the archetypes (see Figure 3). The floor area is equal to 418 m^2, hosting two apartments per floor. The inter-story height is equal to 3.3 m (3.8 m at first story) for H- and M-archetypes, while is equal to 3.0 m for the L-archetypes. Table 5 summarizes the main geometrical characteristics and steel reinforcements details derived from the documental analyses and in situ inspections described in Section 2. The replacement cost (RepC) of the examined archetypes is shown in the last column of Table 4. It has been estimated considering the average cost of construction per square meter of similar new buildings (€730/m^2 according with CIAMI 2014 [30]). Moreover, a further cost for demolition and disposal of materials equal to €135/m^2 [30] has been taken into account, leading to a total replacement cost equal to approximately €865/m^2.

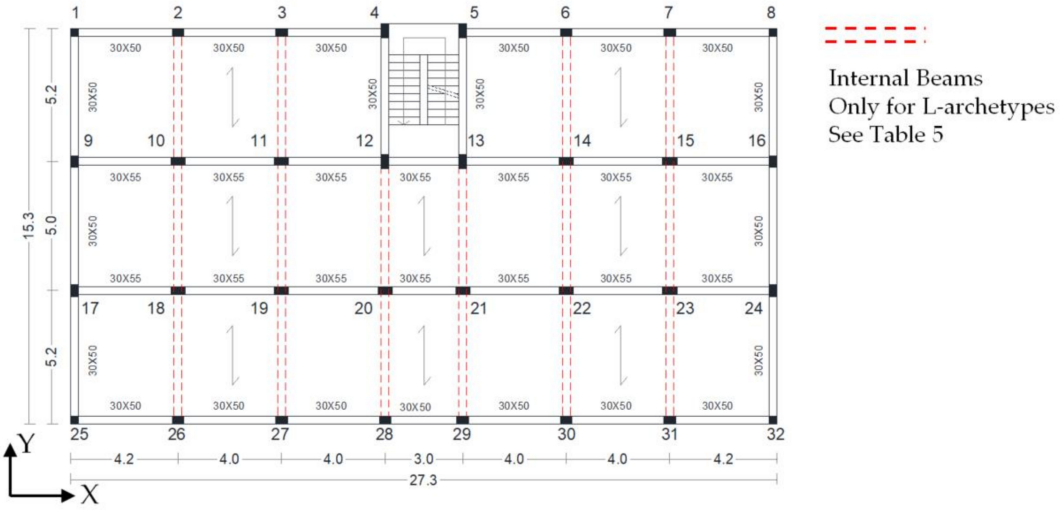

Figure 3. Building layout: structural plan view.

Table 5. Main geometrical characteristics and steel reinforcement details of the selected archetype buildings.

Archetype	Nr. of Frames	Column Section (mm)	Beam Section (mm)	Long. Reinforcements Ratio	Transv. Reinforcements Ratio	Reinforcement Type	Masonry Infills
L, Hr, s, IF	E (X): 2 I (X): 2 E (Y): 2 I (Y): 6	E: 300 × 300–300 × 550 I: 350 × 300–650 × 300 SC: 300 × 650 Cr: 300 × 300	E (X): 300 × 500 I (X): 300 × 550 E (Y): 300 × 500 I (Y): 300 × 400 KB: 300 × 500	B: 0.54–1.07% C: 0.59–1.19%	B: Ø8/150 mm C: Ø8/150 mm SC: Ø8/150 mm	deformed (FeB44k)	100 + 100 mm
L, Mr, s, IF	E (X): 2 I (X): 2 E (Y): 2 I (Y): 6	E: 300 × 300–300 × 450 I: 350 × 300–550 × 300 SC: 300 × 550 Cr: 300 × 300	E (): 300 × 500 I (X): 300 × 550 E (Y): 300 × 500 I (Y): 300 × 400 KB: 300 × 500	B: 0.54–0.94% C: 0.59–1.10%	B: Ø8/150 mm C: Ø8/150 mm SC: Ø8/150 mm	deformed (FeB44k)	100 + 100 mm
M, Hr, k, IF	E (X): 2 I (X): 2 E (Y): 2 I (Y): 0	E: 300 ×3 00–300 × 550 I: 350 × 300–650 × 300 SC: 300 × 650 Cr: 300 × 300	E (X): 300 × 500 I (X): 300 × 550 E (Y):300 × 500 KB: 300 × 500	B: 0.31–0.72% C: 0.58–0.75%	B: Ø6/200 mm C: Ø6/200 mm SC: Ø6/200 mm	smooth (Aq50)	100 + 100 mm
M, Mr, k, IF	E (X): 2 I (dir X): 2 E (Y): 2 I (Y): 0	E: 300 × 300–300 × 450 I: 350 × 300–550 × 300 SC: 300 × 550 Cr: 300 × 300	E (X):300 × 500 I (X):300 × 550 E (Y):300 × 500 KB: 300 × 500	B: 0.31–0.62% C: 0.58–0.70%	B: Ø6/200 mm C: Ø6/200 mm SC: Ø6/200 mm	smooth (Aq50)	100 + 100 mm
M, Lr, k, IF	E (X): 2 I (X): 2 E (Y): 2 I (Y): 0	E: 300 × 300–300 × 350 I: 350 × 300–450 × 300 SC: 300 × 550 Cr: 300 × 300	E (X): 300 × 500 I (X): 300 × 550 E (Y): 300 × 500 KB: 300 × 500	B: 0.31–0.41% C: 0.58–0.68%	B: Ø6/200 mm C: Ø6/200 mm SC: Ø6/200 mm	smooth (Aq50)	100 + 100 mm
H, Hr, k, IF	E (X): 2 I (X): 2 E (Y): 2 I (Y): 0	E: 300 × 300–300 × 550 I: 350 × 300–650 × 300 SC: 300 × 550 Cr: 300 ×3 00	E (X): 300 × 500 I (X): 300 × 550 E (Y): 300 × 500 KB: 300 × 500	B: 0.31–0.72% C: 0.58–0.74%	B: Ø6/250 mm C: Ø6/250 mm SC: Ø6/250 mm	smooth (Aq42)	130 + 100 mm
H, Mr, k, PF	E (X): 2 I (X): 2 E (Y): 2 I (Y): 0	E: 300 × 300–300 × 450 I: 350 × 300–550 × 300 SC: 300 × 500 Cr: 300 × 300	E (X): 300 × 500 I (X): 300 × 550 E (Y): 300 × 500 KB: 300 × 500	B: 0.30–0.62% C: 0.58–0.68%	B: Ø6/250 mm C: Ø6/250 mm SC: Ø6/250 mm	smooth (Aq42)	130 + 100 mm
H, Mr, k, IF	E (X): 2 I (X): 2 E (Y): 2 I (Y): 0	E: 300 × 300 I: 300 × 300 SC: 300 × 300 Cr: 300 × 300	E (X): 250 × 450 I (X): 250 × 450 E (Y): 250 × 450 KB: 250 × 550	B: 0.30–0.60% C: 0.50–0.66%	B: Ø6/250 mm C: Ø6/250 mm SC: Ø6/250 mm	smooth (Aq42)	130 + 100 mm

E: External, I: Internal, Cr: Corner, SC: Staircase; KB: Knee beams, B: Beams; C: Columns.

For what concerns the mechanical properties of concrete, a proper statistical analysis has been carried out. The latter is based on a specific database obtained by assembling the results of compression tests performed by the practitioners performing the seismic assessment on residential RC buildings realized between 1950 and 1990 and located in the Potenza district. The ultimate strength represents the main output data of the compression

tests on core specimens. Unreliable or unclear data have been discarded. As observed by Vona (2014) [31], the value of the compressive strength evaluated during the tests (f_{core}) could be sensibly different from the effective in-situ value (f_c), due to different factors, namely, presence of steel bars in the examined concrete portion, ratio between height (h) and diameter (D) of the examined specimen, sample damage, etc. All that considered, in first approximation, the sample's core strength values have been converted to in-situ values using the following relationship:

$$f_c = (M_{,h/D} \times M_{,dia} \times M_{,a} \times M_{,d}) \times f_{core}, \quad (9)$$

where:

- $M_{,h/D}$ represents the modification factor related to the h/D ratio, equal to $M_{,h/D} = 2/(1.5 + D/h)$;
- $M_{,dia}$ represents the diameter modification factor (1.06 for D = 50 mm, 1.00 for D = 100 mm and 0.98 for D = 150 mm);
- $M_{,a}$ is the modification factor related to the presence of steel bars (ranging from 1.03 to 1.13 as a function of the bar diameter) [32];
- $M_{,d}$ is the modification factor accounting for damage occurring during the extraction activities, equal to 1.06 [33].

Subsequently, the aggregated strength values of the database have been disaggregated, grouping the data in four classes, associated with as many construction periods (pre-1961, 1961–1971, 1972–1981, and post-1981), interspersed with important modifications in the building regulations in force in Italy. The changes in the regulations led inevitably to significant modifications also in the materials quality. In Table 6, the results of the statistical evaluation in terms of concrete strength and in the different construction periods are summarized. For what concerns the steel rebars, the information gathered during the documental analysis has been integrated with the database provided by the STIL software [34] to derive the mechanical properties of steel rebars in the mentioned construction periods. The STIL database is based on the results of 19,140 tensile tests performed on steel rebars used in Italy during the period 1950–2000. Selecting the desired period range and providing, as input, the steel type (smooth or deformed) and, eventually, the specific material category (as a function of the production class and/or regulation's classification in force at the reference period), the software returns the corresponding mechanical properties of the material (yield strength, elongation at fracture, hardening ratio). The mean values and the standard deviations of the yield strength (f_y), obtained for the steel rebars in the mentioned construction periods, are reported in Table 7.

Table 6. Mean value and standard deviation of concrete strength (f_c) in different construction periods.

Statistical Values	Construction Period			
	Pre 1961	**1961–71**	**1972–81**	**Post 1981**
Number of specimens	28	132	264	360
Mean value (N/mm^2)	16.32	19.12	22.21	24.73
Standard Deviation	4.34	10.68	11.32	10.59
C.V.	0.25	0.12	0.08	0.07

Table 7. Yield strength (f_y) of steel rebars in different construction periods.

Statistical Parameter	Construction Period			
	Pre 1961	**1961–71**	**1972–81**	**Post 1981**
Mean Value (N/mm^2)	321.2	369.8	433.1	490.3
Standard Deviation	26.8	33.6	32.5	68.6

The disaggregation of census data obtained using secondary sources of information described in Section 2 highlighted that all the buildings afferent to the H macro-typology

were realized before 1961. As a consequence, the mechanical properties associated with the latter period have been adopted for the numerical models of the archetype buildings representing this macro-typology. Similarly, the mechanical properties determined for post 1981 buildings have been adopted for those referred to the L macro-typology. Finally, for what concerns the M macro-typology, based on the documental analysis, most of the buildings included in this typology (about 80%) have been realized between 1961 and 1971. Only the 20% was built just before or after the latter decade. As a consequence, for the sake of simplicity, the mean mechanical properties of steel and concrete corresponding to the aforementioned construction period (1962–1971) have been adopted for all the numerical models describing the behavior of M-typology.

For what concerns the seismic hazard, all the archetypes are assumed to be located on a medium-soft soil classified as soil type (C), according with the current Italian Seismic Code [18]. For each archetype, the site hazard curve, defined based on the data provided by the INGV (Italian Institute of Geophysics and Volcanology), is expressed in terms of mean annual frequency of exceedance ($MAFE_i$) as a function of the considered IM, namely, the spectral acceleration ($S_{a,i}(T^*)$), corresponding to the average fundamental period of the structure T*.

4.2. Numerical Modeling and Analysis Results

Lumped plasticity models have been implemented in the OpenSees framework [15] to describe the non-linear behavior of the archetype buildings defined in the previous section. The structural elements of the resisting frames have been modeled using the Beam With Hinges (BWH) element, already included in OpenSees. This is a force-based element composed by a central linear elastic region and two discrete plastic hinges on both ends. Such plastic hinges feature a non-linear cyclic behavior according to the modified Ibarra-Medina-Krawinkler deterioration model [35]. Moment–curvature analysis of the critical cross sections of the structural elements (beams and columns) have been performed to derive the inherent skeleton curves, also considering the effect of axial load interaction. Reference to Haselton et al. (2015) [36] has been made to define the degradation parameters for strength and post-capping strength deterioration. Bar slipping has been also taken into account for archetype buildings with smooth rebars (i.e., macro classes H and M), by adopting a proper constitutive law for steel, according with Braga et al. (2012) [37]. It is worth noting that, in this case, the contribution of compression longitudinal rebars has been neglected [38]. Moreover, for RC members featuring smooth rebars, a proper value of the plastic hinge length (H/4 and H/3 for base columns and beams, respectively) has been adopted considering that, although the width of flexural cracks strongly increases due to bond slip effects, these cracks do not spread along the element span during repeated cyclic deformations.

The influence of shear failures on the structural response during the analyses has been explicitly taken into account. All the plastic hinges have been pre-qualified as (i) ductile, in which the shear failure is avoided and the moment-rotational backbone model is not modified, or (ii) shear critical, in which the backbone is reduced after the shear failure, following a softening branch up to zero based on the empirical proposal by Aslani and Miranda (2005) [39].

The model adopted for the joint panel zone of exterior unreinforced joints is the so-called scissors model proposed by Alath and Kunnath (1995) [40]. This model appears very simple from a computational point of view, but also sufficiently accurate in describing the experimental beam–column joint behavior of non-ductile RC frames [41]. In particular, the nonlinear behavior of beam–column joints is modeled using rigid offsets connecting the ends of the beams and columns with two nodes (A and B, respectively) overlapped and located in the center of the panel. Nodes A and B are connected through a rotational spring featuring a single degree of freedom (relative rotation) constitutive model, namely Pinching4 uniaxial material, available in the Opensees framework. The latter model is characterized by a quadri-linear moment vs. rotation relationship, directly related to the

joint shear stress (τj)–shear strain (γj) behavior (see Figure 4). More details can be found in Ricci et al. (2019) [42]. It is worth noting that a negligible influence of interior beam–column joints was highlighted by preliminary analyses. As a consequence, these nodes are not considered in the final models.

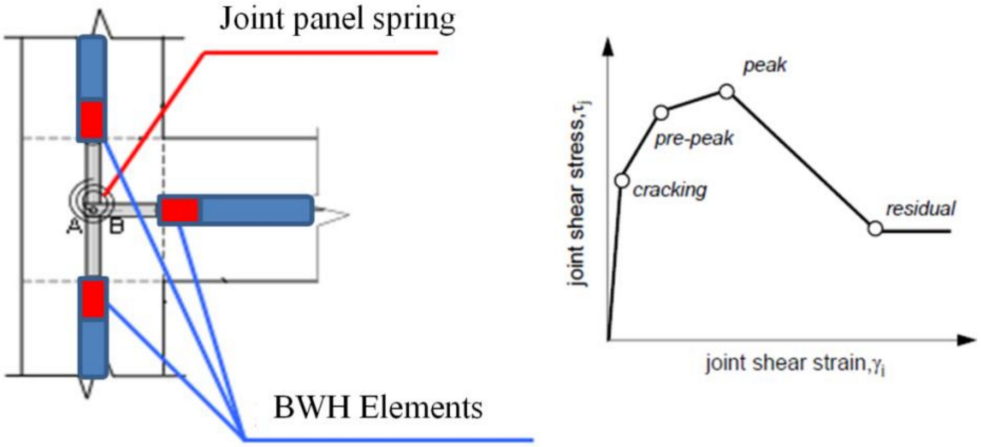

Figure 4. Modeling approach for exterior joint panels.

An equivalent diagonal strut (only in compression) has been adopted to model the masonry infill panels of the examined archetypes. Reference to Sassun et al. (2016) [43] has been made to define the constitutive law of the diagonal struts. In Table 8, the mechanical properties of the constitutive materials composing the (heavy and light) masonry infills are summarized. Specific reduction factors [44] have been considered to opportunely account for the effect of openings, by limiting the strength and lateral stiffness of the panels.

Table 8. Mechanical characteristics of the constitutive materials composing the masonry infill panels.

Brick Type	Mortar	Masonry Panel		
		$_{m0}$ (MPa)	$_{m0}$ (MPa)	E_m (MPa)
Solid bricks thickness 130 mm	Cement + sand	12.00	0.84	6000
Hollow clay bricks thickness 100 mm	Cement + sand	1.20	0.20	1050

The capacity spectrum method (CSM) [45] implementing the N2 approach [46] has been applied to derive the EDPs associated to the reference limit states (ZL, OP, and DC) and the corresponding spectral accelerations at the fundamental period T*. In this optic, non-linear static analyses (push-over) have been performed in the two principal (X- and Y-) directions of each archetype building, considering a linear force distribution (Figures 5–7). It is worth noting that the capacity curves in terms of base shear vs. top displacement have been cut off at a peak strength reduction of about 50% on the negative slope. The failure mode of the H, Mr, k, IF and H, Mr, K, PF archetype buildings is a typical weak-story collapse mechanism located at first story in both cases. However, the differences in terms of columns' dimensions and reinforcement ratios (hence the different response of the involved plastic hinges at first story) produce a different structural behaviour (i.e., different maximum base shear and ultimate displacement) of the two case studies. A mixed-sway mechanism is observed for the H, Hr, k, IF archetype building. As a matter of fact, an initial progressive development of plastic hinges in beams is observed until the occurring of a column-sway mechanism (at the third story), leading to a final soft-story failure mode. For M-archetype buildings, a mixed-sway mechanism is also observed. In the final steps of the analysis, the plastic deformations are mainly concentrated in a single story, different for each case study building due to columns tapering (second story for M, Lr, k, IF, third

story for M, Mr, k, IF, and fifth story for M, Hr, k, IF, respectively). A similar behavior is observed for L-archetype buildings. However, larger over strength ratio (OSR around 1.5) and ductility capacity (on average $\mu_c = 2.3$) have been obtained with respect to those observed for the corresponding M-archetypes (OSR ≈ 1.3 and $\mu_c \approx 1.8$).

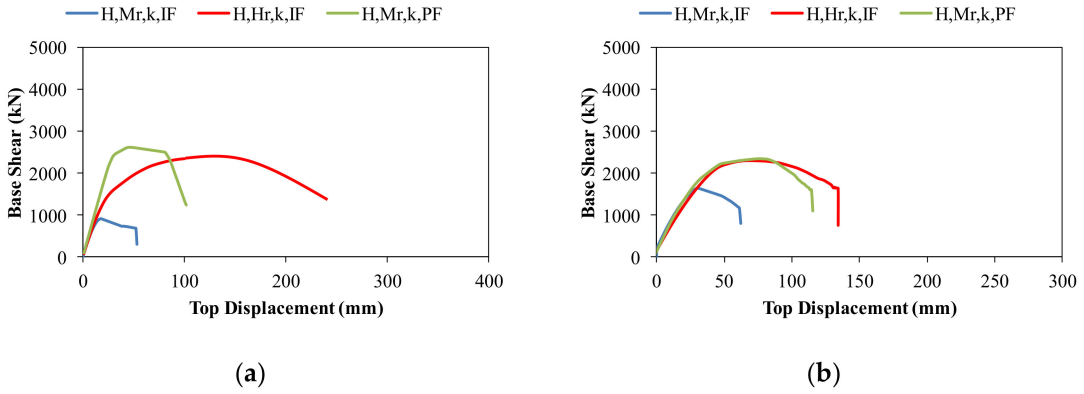

Figure 5. Pushover curves of the selected H-archetype buildings in (**a**) X-direction and (**b**) Y-direction.

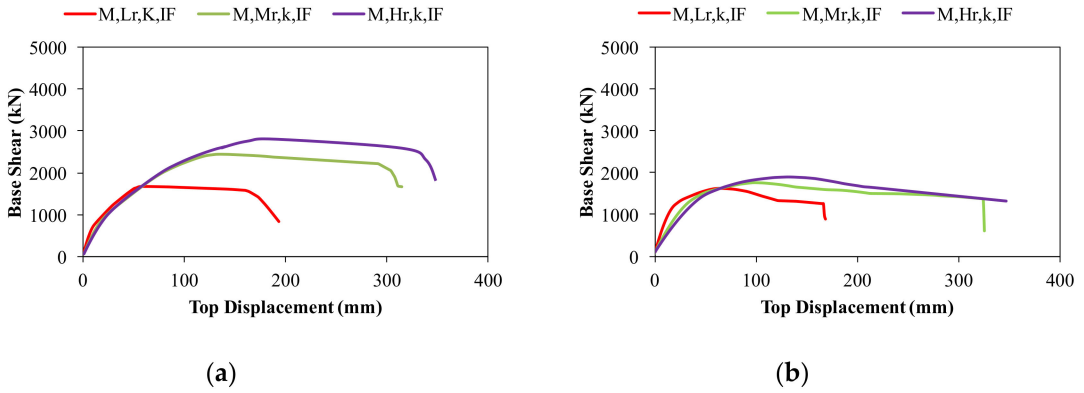

Figure 6. Pushover curves of the selected M-archetype buildings in (**a**) X-direction and (**b**) Y-direction.

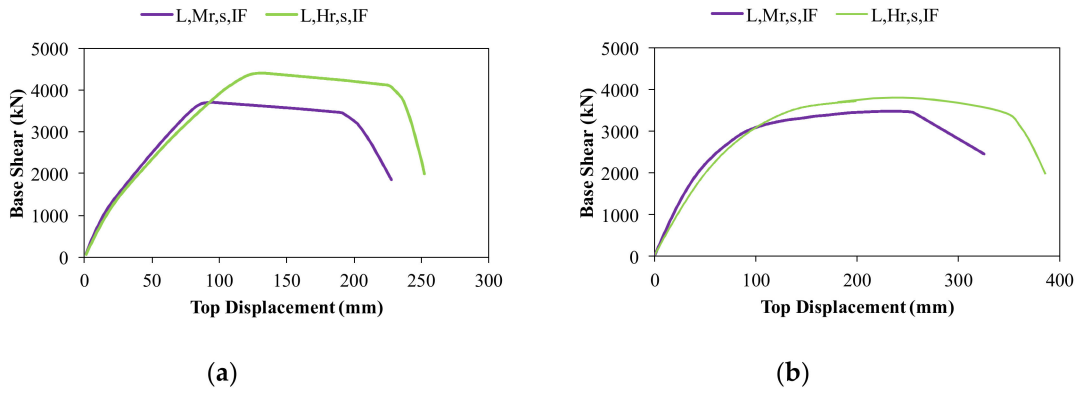

Figure 7. Pushover curves of the selected L-archetype buildings in (**a**) X-direction and (**b**) Y-direction.

Figures 8–10 show the maximum inter story drift profiles (calculated as average between the two principal directions) at the reference limit states (i.e., ZL, OP, and DC) for the H-, M-, and L-archetype buildings, respectively.

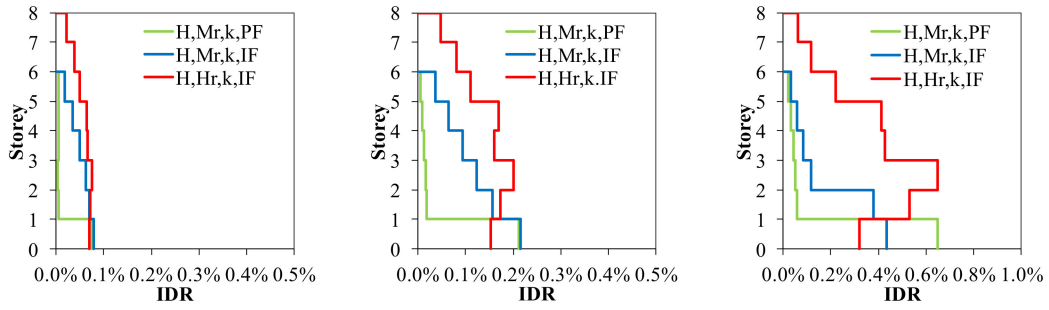

Figure 8. Maximum interstory drift profiles (computed as average between the two principal directions) at (**a**) ZL, (**b**) O, and (**c**) DC performance levels for the H-archetype buildings.

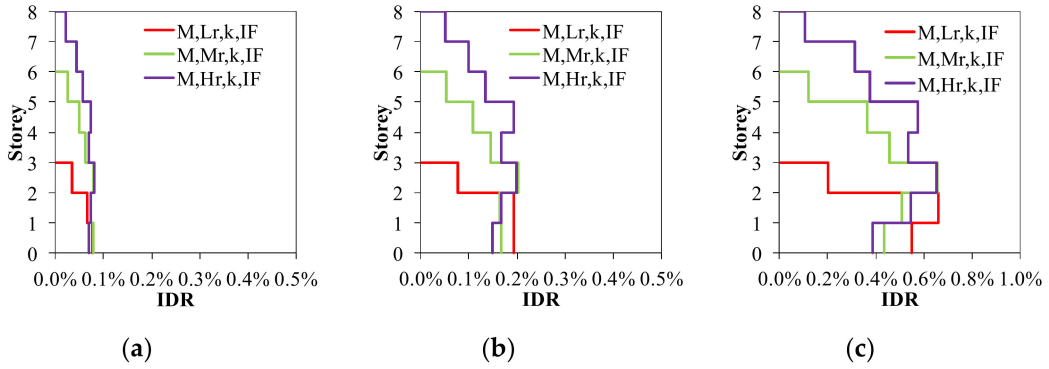

Figure 9. Maximum interstory drift profiles (computed as average between the two principal directions) at (**a**) ZL, (**b**) O, and (**c**) DC performance levels for the M-archetype buildings.

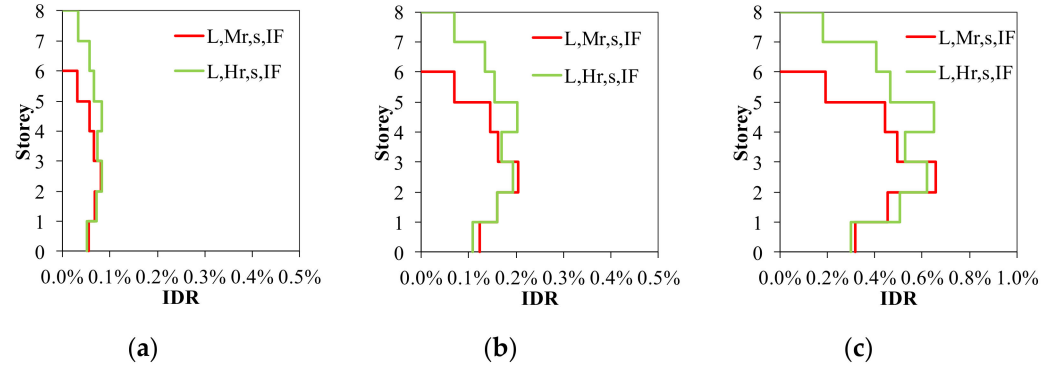

Figure 10. Maximum interstory drift profiles (computed as average between the two principal directions) at (**a**) ZL, (**b**) O, and (**c**) DC performance levels for the L-archetype buildings.

Generally speaking, the inter-story drift profiles show a bulged shape with larger values at the lower and mid stories, increasing with the seismic intensity (from ZL to DC), except for the case studies H, Mr, k, IF and H, Mr, k, PF. As a matter of fact, in these cases, the development of drift (hence damage) is concentrated in the lower stories. This is trivial for the PF case study, considering the effective structural configuration at first story. For what concerns the H, Mr, k, IF archetype, the described condition is related to the limited dimensions of the columns' section (30 × 30 cm continuously along the height of the building) together with the reduced strength and stiffness of the infill panels at the first story (due to large openings).

5. Expected Annual Loss Estimation

The DEAL approach has been performed as described in Section 2, considering three reference limit states, namely ZL, OP, and DC, and adopting suitable story-based loss functions (see Figure 11) derived by Cardone et al. (2020) [4] for first story, typical stories, and top story, assuming a unit RepC equal to €865/m^2 (see Table 9).

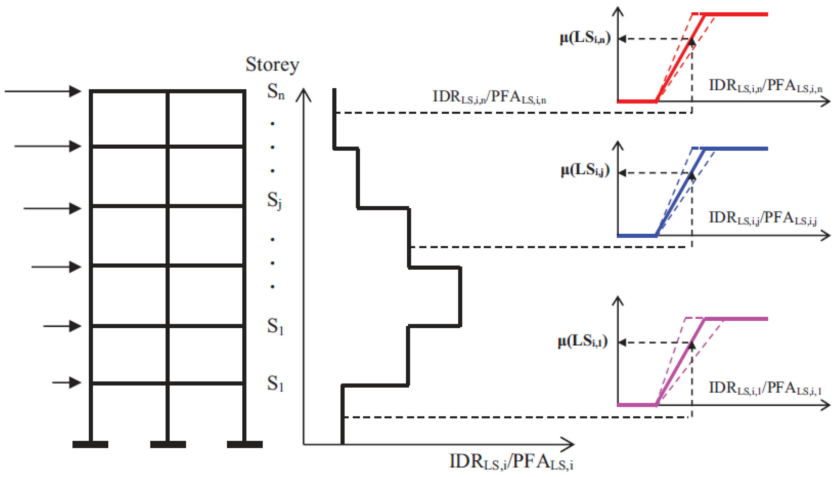

Figure 11. Story-based loss functions: example [3].

Table 9. Story-based loss functions: definition parameters.

Story	Destination of Use	Unit RepC €865/m^2	
		IDR_{in}	IDR_{fin}
First Story	Pilotis-type	0.05%	1.50%
First Story	Partially Infilled	0.05%	1.00%
First Story	Fully Infilled	0.05%	0.8%
Typical Story	Residential	0.05%	0.60%
Top Story	Residential	0.05%	0.40%

Table 10 summarizes the main outputs of the DEAL approach for the examined archetype buildings. In particular, the expected losses (μ) at the selected limit states and the corresponding spectral acceleration (S_a(T*)) are shown. In Table 11, the effective values of direct EAL (EAL_R) in the as-built configuration are provided. Moreover, the values of the indirect component of EAL (EAL_D) are resumed, considering both the LB and UB conditions. The total values of EAL (EAL_R + EAL_D), in the LB and UB, are also provided for each building typology.

Table 10. Main results obtained using the DEAL approach.

Building Typology	T* (sec)	$S_{a,ZL}$ (T*) (g)	$S_{a,OP}$ (T*) (g)	$S_{a,DC}$ (T*) (g)	μ_{ZL} (%RepC)	μ_{OP} (%RepC)	μ_C (%RepC)
L, Hr, s, IF	0.95	0.046	0.104	0.291	3.11	17.91	72.76
L, Mr, s, IF	0.73	0.056	0.129	0.375	2.30	16.84	67.01
M, Hr, k, IF	1.02	0.041	0.090	0.227	2.75	16.75	67.69
M, Mr, k, IF	0.77	0.05	0.107	0.286	2.65	15.52	64.36
M, Lr, k, IF	0.42	0.066	0.178	0.407	2.20	17.73	70.17
H, Hr, k, IF	0.78	0.063	0.135	0.317	2.15	15.30	50.60
H, Mr, k, PF	0.99	0.015	0.036	0.114	0.30	1.85	7.19
H, Mr, k, IF	0.61	0.068	0.119	0.235	1.63	10.86	21.94

Table 11. EAL values derived from DEAL approach.

Building Typology	EAL_R (%RepC)	$EAL_{R,retrofit}$ (%RepC)	$EAL_{D,LB}$ (%RepC)	$EAL_{D,UB}$ (%RepC)	$EAL_{T,LB}$ (%RepC)	$EAL_{T,LB}$ (%RepC)
L, Hr, s, IF	1.76	1.00	0.14	0.22	1.9	1.98
L, Mr, s, IF	1.68	1.00	0.13	0.21	1.81	1.89
M, Hr, k, IF	1.96	1.00	0.17	0.26	2.13	2.22
M, Mr, k, IF	2.03	1.00	0.16	0.25	2.19	2.28
M, Lr, k, IF	2.75	1.50	0.19	0.31	2.94	3.06
H, Hr, k, IF	1.3	0.50	0.17	0.26	1.47	1.56
H, Mr, k, PF	0.62	0.50	0.08	0.12	0.7	0.74
H, Mr, k, IF	1.27	0.50	0.16	0.25	1.43	1.52

The results obtained in terms of EAL_R are directly related to the structural response of the examined buildings during the non-linear analyses. Indeed, the effective shape of the drift profiles directly affects the distribution of damage (and monetary losses) along the height of the buildings. For the H-archetypes, EAL_R values of the order of 1.3% have been obtained in the Infilled Frame configuration (H, Hr, k, IF and H, Mr, k, IF), while a lower value has been obtained for the Pilotis Frame archetype building (H, Mr, k, PF). As a matter of fact, the concentration of drifts (hence damage and losses) at the first story of the PF archetype significantly reduces the value of EAL_R. Similarly, the almost uniform distribution of IDR and damage observed for the M-archetypes produces larger values of EAL_R, of about 2.25% on average. This consideration is somehow emphasized for the M, Lr, k, IF archetype, where the IDR values appears constant for the 2/3 of the building height, leading to the peak value of EAL_R (2.75%). Finally, normalized spectral acceleration ($S_a(T^*)/S_a(T^*)_{ZL}$) being equal, the enhanced performances of the L-archetypes determinates a reduction of the direct monetary losses with respect to M-archetypes, leading to lower values of EAL_R (of approximately 25%, on average). Values of EAL_D of the order of 0.15% and 0.25% have been obtained for the LB and UB condition, respectively. Considerations similar to those reported for the direct component of EAL can be made with reference to the EAL_D values obtained for each macro-typology (H-, M-, and L-). Generally speaking, the contribution of the indirect component of EAL is of the order of 15% (10%) in the UB (LB) condition.

In order to have a general understanding of the potential socio-economic effects of the seismic scenarios at territorial scale, the EAL_T values obtained for the specific archetype buildings have been monetized with respect to the actual replacement cost. Subsequently, the monetary expected annual loss of the two compartments has been calculated by multiplying, for each building typology, the EAL_T value for the total number of elements of this category. As reported in Table 12, the total expected annual loss of the entire "virtual" compartments (i.e., area's expected annual loss, AEAL) amounts to approximately 540 millions of Euro (average between LB and UB condition). To give some reference for the mentioned value, the latter can be compared to the area's total income (ATI) obtained multiplying the per capita income (PCI) measured in the examined area in the last year (equal to €16,522 [22]), by the total number of occupants (equal to 4330). All that considered, the ratio between AEAL and ATI is equal to approximately 7.5 (540 millions divided by 71.5 million Euros). In other words, the average economic loss that is expected to accrue every year in the examined area, considering both the repair costs and the indirect costs related to downtime, is seven times larger than the annual average income of all the inhabitants. In practice, if only private resources were used to recover the economic losses and assuming that each owner gets a mortgage with an annual payment equal to 1/5 of his PCI (approximately €3300), 40 years are needed to pay back the economic losses accrued in only one year.

Table 12. Monetized EAL values estimated for the examined "virtual" compartments.

Building Typology	$EAL_{T,LB}$ (€)	$EAL_{T,UB}$ (€)	$EAL_{R,as\text{-}built}$ (€)	$EAL_{R,retrofitted}$ (€)	EAL_R (€)
L, Hr, s, IF	38,011,400	39,611,880	35,210,560	20,006,000	15,204,560
L, Mr, s, IF	19,321,750	20,175,750	17,934,000	10,675,000	7,259,000
M, Hr, k, IF	152,188,500	158,619,000	140,042,000	71,450,000	68,592,000
M, Mr, k, IF	102,864,300	107,091,600	95,349,100	46,970,000	48,379,100
M, Lr, k, IF	19,009,573	19,785,474	17,781,063	9,698,761	8,082,301
H, Hr, k, IF	58,817,640	62,418,720	52,015,600	20,006,000	32,009,600
H, Mr, k, PF	17,934,000	18,958,800	15,884,400	12,810,000	3,074,400
H, Mr, k, IF	122,122,000	129,808,000	108,458,000	42,700,000	65,758,000
AEAL	530,269,163	556,469,224	482,674,723	234,315,761	-
AEAL	-	-	-	-	248,358,961

Recently, the Italian 2019 Financial Law [47], introduced the so-called "Sisma Bonus" providing incentives granted in the form of tax credits. Incentives ranges from 50% to 85% of the retrofit intervention's total cost. The incentives system is directly related to the risk classes defined in the Italian seismic risk classification guidelines [12], associated to specific ranges of EAL (see Table 13). A 50% incentive can be obtained by implementing retrofit interventions without class improvement with respect to the state of the art. On the other hand, 75% and 85% incentives can be obtained in case of improvement of one or two seismic risk classes, respectively. In any case, the maximum retrofitting expenditure amounts to €96,000 per property unit (single family house, apartment, etc.). Moreover, following the recent COVID19 pandemic, a special "Super Bonus" [48] up to 110% has been issued, with maximum retrofitting expenditure per property unit raised up to €136,000. Besides the tax incentives, the assignment of credit solution is also allowed. In practice, the accrued credit can be transferred to the involved construction firm or even to third parties (financial institutions, banks, lenders), thus limiting or even avoiding the economic burden for the stakeholders. It is worth noting that, in line with the Italian seismic risk classification guidelines, reference to the direct component of EAL (EAL_R) has been made in what follows. For each building typology, the fifth column of Table 12 provides the monetary EAL_R values obtained considering potential retrofit interventions aimed at the improvement of two seismic classes with respect to the as-built condition. The reduction of EAL_R for each building typology ($\Delta EAL_R = EAL_{R,as\text{-}built} - EAL_{R,retrofit}$) is also reported (last column of Table 12). The total variation of the EAL_R ($\Delta AEAL_R$) is equal to €248,358,961. On the other hand, assuming that all the buildings' owners exploit the maximum retrofit expenditure amount (i.e., 136,000 per property unit), the total cost of the intervention is equal to €233,920,000. Therefore, only one year would be sufficient to pay back the entire amount of the financial resources involved in the seismic protection improvement of the examined area's built heritage. Moreover, if the mentioned interventions are implemented, the reduction of economic losses that is expected every year in the examined territorial area is of the order of 250 million Euros, about 3.5 times the Area's Total Income.

Table 13. Reference values of EAL_R for seismic risk classes definition [8].

Expected Annual Loss (EAL_R)	Class
≤0.50%	A+
0.50%–1.0%	A
1.0%–1.5%	B
1.5%–2.5%	C
2.5%–3.5%	D
3.5%–4.5%	E
5.5%–7.5%	F
>7.5%	G

6. Conclusions

A simplified approach for the seismic loss assessment of RC buildings at urban scale is proposed herein based on the DEAL methodology [14].

Two residential compartments of the city of Potenza (Italy) have been examined. After a preliminary identification of the prevalent building typologies, a certain number of archetype buildings, featuring the geometrical, material and structural peculiarities of the mentioned building typologies, have been defined and modeled in the Opensees framework. The N2 method has been performed to derive the main parameters for the DEAL approach application. Expected direct monetary losses and the direct component of the EAL (EAL_R) have been derived for each building typology. Similarly, the indirect component of EAL (EAL_D) has been calculated. To have a general understanding of the socio-economic impacts of the seismic scenarios at territorial scale, the value of the Area's Expected Annual Loss has been estimated in the as-built configuration. This value has been compared with the area's total income of the actual population, obtaining a ratio equal to approximately 7.5.

In the last part of the present study, considering the recent economic actions undertaken by the Italian Government to gradually reduce the seismic vulnerability of the existing building stock, a global retrofit intervention, aimed at the improvement of two seismic risk classes for all the buildings located in the examined area, has been considered. Generally speaking, the mentioned global intervention could significantly reduce the direct EAL of about 50%, from 480 to 234 million Euros. Moreover, the maximum total amount of the global retrofit intervention is equal to approximately 230 million Euros, thus of the same order of the total reduction in terms of expected annual loss. In other words, the pay-back period (i.e., period of time necessary to recover the cost of the investment) is about one year. More case studies are needed to definitively assess the applicability of the proposed simplified approach. Moreover, other building typologies (public buildings, masonry buildings) should be included to derive a global understanding and a complete evaluation of the socio-economic impact at the territorial scale. Finally, specific retrofit interventions should be designed for each building typology, in order to precisely estimate the actual economic expenses and the effective seismic performances in the retrofitted configuration.

Author Contributions: Conceptualization, A.F., D.C. and M.V.; methodology, A.F.; software, A.F.; validation, A.F.; formal analysis, A.F.; investigation, A.F.; resources, A.F.; data curation, A.F. and G.P.; writing—original draft preparation, A.F.; writing—review and editing, A.F., D.C., M.V., and G.P.; visualization, A.F.; supervision, A.F., D.C. and M.V.; project administration, A.F., D.C. and M.V.; funding acquisition, D.C. and M.V. All authors have read and agreed to the published version of the manuscript.

Funding: This research was funded by the PON-AIM 2014–2020 project supported by the Italian Ministry of University and Public Instruction.

Data Availability Statement: Istat Database at https://www.istat.it/.

Acknowledgments: This research has been developed within the PON-AIM 2014-2020 project, "Attraction and International Mobility", Line 1, supported by the Italian Ministry of University and Public Instruction.

Conflicts of Interest: The authors declare no conflict of interest.

References

1. Liang, L.; David, Y.Y.; Dan, M.F. Determining target reliability index of structures based on cost optimization and acceptance criteria for fatality risk. In *ASCE-ASME Journal of Risk and Uncertainty in Engineering Systems, Part A: Civil Engineering*; American Society of Civil Engineers: Reston, VA, USA, 2021; Volume 7.
2. Cardone, D.; Flora, A.; Manganelli, B. Cost-benefit analysis of different retrofit strategies following a displacement based loss assessment approach: A case study. In Proceedings of the Tenth U.S. National Conference on Earthquake Engineering Frontiers of Earthquake Engineering, Anchorage, AL, USA, 21–25 July 2014. [CrossRef]

3. Vona, M.; Manganelli, B.; Tataranna, S.; Anelli, A. An optimized procedure to estimate the economic seismic losses of existing reinforced concrete buildings due to seismic damage. *Buildings* **2018**, *8*, 144. [CrossRef]
4. Cardone, D.; Perrone, G.; Flora, A. Displacement-Based Simplified Seismic Loss Assessment of Pre-70S RC Buildings. *J. Earth. Eng.* **2020**, *24*, 82–113. [CrossRef]
5. Porter, K.A. An overview of PEER's performance-based earthquake engineering methodology. In Proceedings of the Ninth International Conference on Applications of Probability and Statistics in Engineering, San Francisco, CA, USA, 6–9 July 2003.
6. Porter, K.A.; Beck, J.L.; Shaikhutdinov, R.V. Simplified estimation of economic seismic risk for buildings. *Earth. Spectra* **2004**, *20*, 1239–1263. [CrossRef]
7. Krawinkler, H. *Van Nuys Hotel Building Testbed Report: Exercising Seismic Performance Assessment*; Pacific Earthquake Engineering Research Center College of Engineering University of California: Berkeley, CA, USA, 2005.
8. Anelli, A.; Hidalgo, S.S.C.; Vona, M.; Tarque, N.; Laterza, M. A proactive and resilient seismic risk mitigation strategy for existing school buildings. *Struct. Infrastruct. Eng.* **2019**, *15*, 137–151. [CrossRef]
9. Vona, M. Proactive Actions Based on a Resilient Approach to Urban Seismic Risk Mitigation. *Open Constr. Build. Technol. J.* **2020**, *14*, 321–335. [CrossRef]
10. Sullivan, T.J.; Calvi, G.M. Considerations for the seismic assessment of buildings using the direct displacement-based assessment approach. In Proceedings of the ANIDIS Conference, Bari, Italy, 18–22 September 2011.
11. Ramirez, C.M.; Miranda, E. *Building Specific Loss Estimation Methods Tools for Simplified Performance Based Earthquake Engineering*; Technical Report No. 171; John A. Blume Earthquake. Engineering Center: Palo Alto, CA, USA, May 2009.
12. *Linee Guida per la Classificazione del Rischio Sismico delle Costruzioni*; numero 58 del; Decreto Ministeriale: Rome, Italy, 2017.
13. Perrone, G.; Cardone, D.; O'Reilly, G.J.; Sullivan, T.J. Developing a direct approach for estimating expected annual losses of Italian buildings. *J. Earth. Eng.* **2019**, 1–32. [CrossRef]
14. Cardone, D.; Sullivan, T.J.; Gesualdi, G.; Perrone, G. Simplified estimation of the expected annual loss of reinforced concrete buildings. *Earth. Eng. Struct. Dyn.* **2017**, *46*, 2009–2032. [CrossRef]
15. McKenna, F. OpenSees: A Framework for Earthquake Engineering Simulation. *Comput. Sci. Eng.* **2011**, *13*, 58–66. [CrossRef]
16. Cardone, D.; Flora, A.; Picione, M.D.L.; Martoccia, A. Estimating direct and indirect losses due to earthquake damage in residential RC buildings. *Soil Dyn. Earthq. Eng.* **2019**, *126*, 105801. [CrossRef]
17. Vamvatsikos, D. Derivation of new SAC/FEMA performance evaluation solutions with second-order hazard approximation. *Earthq. Eng. Struct. Dyn.* **2013**, *42*, 1171–1188. [CrossRef]
18. *Norme Tecniche per le Costruzioni*; NTC2018; Ufficio Pubblicazione Leggi E Decreti: Rome, Italy, 2018.
19. Cardone, D.; Perrone, G. Damage and Loss Assessment of Pre-70 RC Frame Buildings with FEMA P-58. *J. Earthq. Eng.* **2016**, *21*, 1–39. [CrossRef]
20. Applied Technology Council. *Next-Generation Seismic Performance Assessment for Buildings*; FEMA P-58-1 Federal; Emergency Management Agency: Washington, DC, USA, 2012.
21. Cardone, D.; Flora, A. Multiple inelastic mechanisms analysis (MIMA): A simplified method for the estimation of the seismic response of RC frame buildings. *Eng. Struct.* **2017**, *145*, 368–380. [CrossRef]
22. Italian National Statistics Institute (ISTAT). *15th National Census on Buildings and Population*; Italian National Statistics Institute (ISTAT): Rome, Italy, 2014. (In Italian)
23. Gizzi, F.T.; Masini, N. Historical earthquakes and damage patterns in Potenza (Basilicata, Southern Italy). *Ann. Geophys.* **2007**, *50*, 676–687.
24. Chiauzzi, L.; Masi, A.; Mucciarelli, M.; Vona, M.; Pacor, F.; Cultrera, G.; Gallovič, F.; Emolo, A. Building damage scenarios based on exploitation of Housner intensity derived from finite faults ground motion simulations. *Bull. Earthq. Eng.* **2011**, *10*, 517–545. [CrossRef]
25. Grunthal, G. *European Macroseismic Scale (EMS–98)*; Cahiers du Centre Européen de Géodynamique et de Séismologie: Luxembourg, 1998.
26. Dolce, M.; Kappos, A.; Masi, A.; Penelis, G.; Vona, M. Vulnerability assessment and earthquake damage scenarios of the building stock of Potenza (Southern Italy) using Italian and Greek methodologies. *Eng. Struct.* **2006**, *28*, 357–371. [CrossRef]
27. Brzev, S.; Scawthorn, C.; Charleson, A.W.; Jaiswal, K. *Interim Overview of GEM Build-ing Taxonomy V2.0*; GEM Technical Report Version 1.0; GEM Foundation: Pavia, Italy, 2013.
28. Flora, A.; Iacovino, C.; Cardone, D.; Vona, M. *Typological Inventory of Residential Reinforced Concrete Buildings for the City of Potenza*; Lecture Notes in Computer Science: Cagliari, Italy, 2020; pp. 899–913.
29. Masi, A.; Vona, M. Vulnerability assessment of gravity-load designed RC buildings: Evaluation of seismic capacity through non-linear dynamic analyses. *Eng. Struct.* **2012**, *45*, 257–269. [CrossRef]
30. Collegio degli ingegneri e degli architetti di Milano. *Prezzo Tipologie Edilizie. 2014*; Tipografica del Genio Civile: Rome, Italy, 2014. (in Italian)
31. Vona, M. A Review of Experimental Results about In Situ Concrete Strength. *Adv. Mater. Res.* **2013**, *773*, 278–282. [CrossRef]
32. Masi, A.; Chiauzzi, L. An experimental study on the within-member variability of in situ concrete strength in RC building structures. *Constr. Build. Mater.* **2013**, *47*, 951–961. [CrossRef]
33. Applied Technology Council. *Commentary on the Guidelines for the Seismic Rehabilitation of Buildings*; FEMA 274-NEHRP; Federal Emergency Management Agency: Washington, DC, USA, 1997.

34. Verderame, G.M.; Ricci, P.; Esposito, M.; Manfredi, G. *STIL v1.0–Software Per La Carat-Terizzazione Delle Proprietà Meccaniche Degli Acciai Da c.a. Tra il 1950 e il 2000*; ReLUIS: Naples, Italy, 2012.
35. Ibarra, L.F.; Medina, R.A.; Krawinkler, H. Hysteretic models that incorporate strength and stiffness deterioration. *Earthq. Eng. Struct. Dyn.* **2005**, *34*, 1489–1511. [CrossRef]
36. Haselton, C.B.; Liel, A.B.; Lange, S.T.; Deierlein, G.G. *Beam-Column Element Model Cal-Ibrated for Predicting Flexural Response Leading to Global Collapse of RC Frame Buildings*; Pacific Earthquake Engineering Research Center: Berkeley, CA, USA, 2008.
37. Braga, F.; Gigliotti, R.; Laterza, M.; D'Amato, M.; Kunnath, S.F. Modified Steel Bar Model Incorporating Bond-Slip for Seismic Assessment of Concrete Structures. *J. Struct. Eng.* **2012**, *138*, 1342–1350. [CrossRef]
38. Gesualdi, G.; Viggiani, L.R.S.; Cardone, D. Seismic performance of RC frame buildings accounting for the out-of-plane behavior of masonry infills. *Bull. Earthq. Eng.* **2020**, *18*, 1–39. [CrossRef]
39. Aslani, H.; Miranda, E. *Probabilistic Earthquake Loss Estimation and Loss Disaggregation in Buildings*; Report No., 157; The John A. Blume Earthquake Engineering Center Department of Civil and Environmental Engineering Stanford University: Palo Alto, CA, USA, June 2005.
40. Alath, S.; Kunnath, S.K. *Modelling Inelastic Shear Deformations in RC Beam-Column Joints*; American Society of Civil Engineers: Boulder, CO, USA, 1995.
41. De Risi, M.T.; Ricci, P.; Verderame, G.M.; Manfredi, G. Experimental assessment of un-reinforced exterior beam-column joints with deformed bars. *Eng. Struct.* **2016**, *112*, 215–232. [CrossRef]
42. Ricci, P.; Manfredi, V.; Noto, F.; Terrenzi, M.; De Risi, M.T.; Di Domenico, M.; Camata, G.; Franchin, P.; Masi, A.; Mollaioli, F.; et al. RINTC-e: Towards seismic risk assessment of existing residential reinforced concrete buildings in Italy. In Proceedings of the 7th International Conference on Computational Methods in Structural Dynamics and Earthquake Engineering, Crete, Greece, 24–26 June 2019. [CrossRef]
43. Sassun, K.; Sullivan, T.J.; Morandi, P.; Cardone, D. Characterising the in-plane seismic performance of infill masonry. *Bull. New Zealand Soc. Earthq. Eng.* **2016**, *49*, 100–117. [CrossRef]
44. Cardone, D.; Perrone, G.; Piesco, V. Developing collapse fragility curves for base-isolated buildings. *Earthq. Eng. Struct. Dyn.* **2019**, *48*, 78–102. [CrossRef]
45. Richard, W.N. *Seismic Evaluation and Retrofit of Concrete Buildings*; Report No. SSC 96-01; Applied Technology Council (ATC): Redwood City, CA, USA, November 1996.
46. *Eurocode 8: Design of Structures for Earthquake Resistance–Part 1: General Rules, Seismic Actions and Rules for Buildings, German Version*; EN 1998-1:2004; European Committee for Standardization: Brussels, Belgium, December 2010.
47. *In Bilancio di Previsione dello Stato per l'Anno Finanziario 2019 e Bilancio Pluriennale per il Triennio 2019–2021 (Legge di Bilancio 2019)*; Law 145/2018,.n.302 del; Gazzetta U_ciale della Repubblica Italiana: Roma, Italy, 2018. (In Italian)
48. *Recante Misure Urgenti in Materia di Salute, Sostegno al Lavoro e all'Economia, Nonche' di Politiche Sociali Connesse all'Emergenza Epidemiologica da COVID-19*; Law 77/2020, n.180 del; Gazzetta U_ciale della Repubblica Italiana: Roma, Italy, 2020. (In Italian)